

T H E U N I V E R S I T Y O F M I C H I G A N

COLLEGE OF ENGINEERING

Department of Engineering Mechanics

Technical Report

THE KINEMATICS OF SOILS

R. M. Haythornthwaite

ORA Project 04403

under contract with:

DEPARTMENT OF THE ARMY
ORDNANCE TANK-AUTOMOTIVE COMMAND
DETROIT ORDNANCE DISTRICT
CONTRACT NO. DA-20-018-ORD-23276
DETROIT, MICHIGAN

administered through:

OFFICE OF RESEARCH ADMINISTRATION ANN ARBOR

August 1962

ACKNOWLEDGEMENTS

This paper reports work sponsored by the Land Locomotion Laboratory, U. S. Army Ordnance Arsenal, Detroit, under Contract DA-20-018-ORD-23276 with The University of Michigan. The study was started while the author was at the University of Cambridge. Facilities for carrying out the triaxial test were provided by Professor T. H. Wu of the Department of Civil Engineering, Michigan State University. Professor Wu suggested the use of an internal vacuum rather than external pressure in order to simplify observation of the shape changes in the specimen.

TABLE OF CONTENTS

	Page
LIST OF FIGURES	vii
SUMMARY	1
I. INTRODUCTION	2
Coulomb Glide	3
II. AXIAL SYMMETRY	6
III. THE TRIAXIAL TEST	9
IV. EXPERIMENTAL EVIDENCE	18
REFERENCES	21

LIST OF FIGURES

Figure		Page
1	(a) A typical stress state meeting the Coulomb criterion of yield. The largest Mohr circle touches the failure lines AC and AD; (b) Orientation of the principal directions of strain for slip on planes with stress state C, Fig. 1a; (c) Orientation of the principal directions of strain for slip on planes with stress state D, Fig. 1a.	4
2	Unit vectors for two sets of orthogonal axes.	7
3	The triaxial test.	9
4	Strain states for the triaxial test.	11
5	Regions of deformation with axial symmetry.	14
6	Distortion of an initially square grid for deformation with axial symmetry.	15
7	Distortion of an initially square grid for an alternative velocity field.	17
8	Load-deflection curve from a triaxial test on Ottawa sand.	19
9	Average rates of radial expansion for two increments during the failure of a specimen of Ottawa sand in compression.	20

SUMMARY

A continuum model which provides an adequate representation of the mechanical behavior of a random granular medium such as soil has yet to be discovered. In this paper one candidate—the material which deforms by glide on the critical Coulomb friction planes—is used to analyze the kinematics of deformation under conditions of axial symmetry. As in plane strain, the principal directions of stress and strain rate do not necessarily coincide. A detailed analysis is given for the triaxial test and the predicted displacements are compared with some test results for a sand.

I. INTRODUCTION

The kinematic consequences of the concepts of soil deformation usually associated with the names of Coulomb and Rankine have never been fully explored, and it is not known whether they can be used to describe the observed behavior of soils. This question is of some significance because recent work on the theory of plasticity has shown that a specification of the nature of the deformations which may accompany a given stress state can be the key to the establishment of the uniqueness of the solutions to boundary value problems without the need for reference to secondary effects such as strain hardening, geometry changes, etc. In this paper, the kinematics of one type of Coulomb glide is investigated for axial symmetry of the stresses, and certain experimental observations are presented.

In his pioneer work on the stability of retaining walls, Coulomb thought in terms of rupture along a single critical surface of sliding on which a nominal coefficient of friction was exceeded.¹ Rankine² extended this idea by introducing the concept of many parallel planes of incipient slip in the uniform stress case. Neither author attempted to make use of kinematic conditions in their subsequent analyses. It can be shown, however, that the existence of incipient planes of sliding is not enough to establish the uniqueness of the associated stress states in mixed boundary value problems and that, without further kinematic restrictions, many alternative stress states are equally likely. There is the possibility that stress distributions in granular media are not intrinsically unique even though consistent values can be obtained for surface tractions, but we do not wish to adopt this point of view until the last possibility for restricting the stress distributions through kinematic conditions has been exhausted.

Uniqueness of stresses can be imposed by adopting a modified material model. While retaining the Coulomb criterion of yielding, Drucker and Prager³ have suggested the use of a stress-strain law of the ideally plastic type, for which theorems are available which establish uniqueness of the stresses. Unfortunately the concept of sliding on the critical planes must then be replaced by the concept of an expanding layer and the volume changes predicted by this theory far exceed any which have been observed, even momentarily. There is, however, the possibility that the true extent of the dilation rates at the instant of failure is obscured by elastic effects and by volume changes in the remainder of the material. Drucker, Gibson and Henkel⁴ and Jenike and Shield⁵ have introduced the model of a strain hardening plastic solid in order to allow smaller or vanishing dilations. These authors retain the assumption that the principal directions of stress and strain coincide. An unfortunate consequence is that the computed directions of maximum shear strain no longer coincide with the observed slip planes, which prevents this alternative from being regarded as entirely satisfactory.

COULOMB GLIDE

In the Coulomb theory, resistance to failure is regarded as essentially frictional in nature. The shear stress τ_0 causing slip on any plane is taken as the sum of a constant value, termed the cohesion, and an additional amount that is proportional to the normal pressure acting across the plane. Thus

$$\tau_0 = c - \sigma \tan \phi \quad (1)$$

in which c is the cohesive stress, σ denotes the tensile stress across the plane, and ϕ is the angle of friction of the material. This relationship follows a straight line in the $\sigma - \tau$ plane (Fig. 1a), in which the representation of stress at a point (Mohr⁶) can also be drawn. A stress state for which failure is incipient on some plane will be represented by a circle touching the failure line, such as that shown in Fig. 1a. From the geometry of the triangle ABC,

$$\sigma_3 - \sigma_1 = 2c \cos \phi - (\sigma_1 + \sigma_3) \sin \phi \quad (2)$$

in which σ_1 and σ_3 are principal stresses. The intermediate principal stress σ_2 , where $\sigma_1 \leq \sigma_2 \leq \sigma_3$, does not appear in the relationship.

All experimental data for sands obtained for the direct shear, ring shear (torsion), and triaxial tests are consistent with the assumption of failure on the critical Coulomb friction planes, as expressed in Eq. (1); however, in none of these tests is a completely general state of combined stress reached. Two of the principal stresses are always equal if a homogeneous state of stress is assumed in the specimens. Results obtained with a combined compression and torsion machine⁷ indicate that the Coulomb criterion of failure may not be followed for complex stress states in which the intermediate principal stress differs from the maximum and minimum principal stresses. Some question remains, however, as to whether the stress state achieved in the latter tests was in fact homogeneous, and there is still a reasonable chance that the Coulomb theory will be shown to provide an adequate model for all combinations of stress.

If sliding can occur along the failure planes, the principal directions of stress and strain do not necessarily coincide. In Fig. 1b, the nature of the strain is indicated for planes on which the stress state corresponds to point C, Fig. 1a. It is a property of the Mohr circle that the angle subtended at B, Fig. 1a, is twice the angle of inclination of the plane on which the corresponding stresses act. Thus in Fig. 1b let the critical plane corresponding to stress state C, Fig. 1a, be EF. Since the extension rate will be zero along the plane and since there is no volume change in the plane, the principal directions of the strain will subtend 45° to EF. The principal directions of strain will

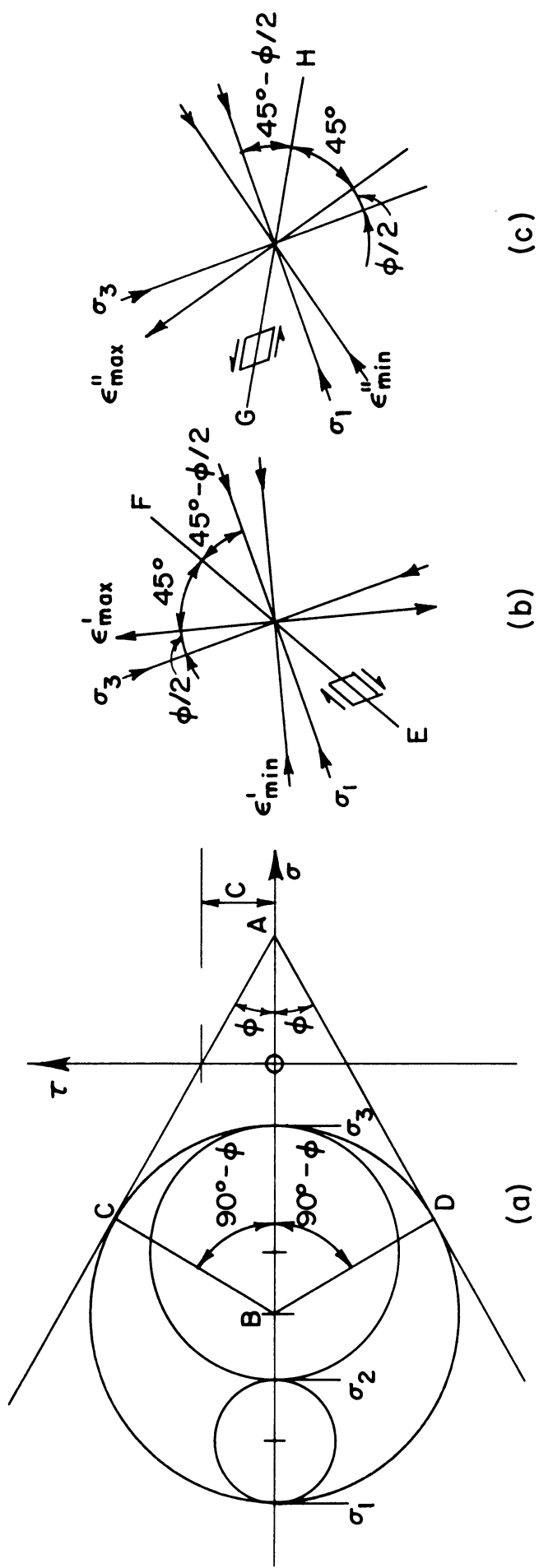


Fig. 1. (a) A typical stress state meeting the Coulomb criterion of yield. The largest Mohr circle touches the failure lines AC and AD; (b) Orientation of the principal directions of strain for slip on planes with stress state C, Fig. 1a; (c) Orientation of the principal directions of strain for slip on planes with stress state D, Fig. 1a.

deviate $\phi/2$ from the principal directions of stress. In the same fashion slip on planes for which the stress state is represented by point D, Fig. 1a, will give rise to strain with principal direction as shown in Fig. 1c. Simultaneous slip on both sets of planes—EF, Fig. 1b, and GH, Fig. 1c—is deemed possible and the principal directions of strain can be found by superposition. Denoting the angle of departure of a principal direction of strain from the closest principal direction of stress by $\alpha/2$,

$$\tan\alpha = \tan\phi \cdot \frac{e'_{\max} - e''_{\max}}{e'_{\max} + e''_{\max}} \quad (3)$$

Now E'_{\max} and E''_{\max} are both intrinsically positive because there is no volume expansion during slip; hence

$$1 \geq \frac{e'_{\max} - e''_{\max}}{e'_{\max} + e''_{\max}} \geq -1 \quad (4)$$

Thus α lies in the range

$$\phi \geq \alpha \geq -\phi \quad (5)$$

DeJong has derived this same result, but by a different method.⁸

II. AXIAL SYMMETRY

In axially symmetric problems the plane-strain motion associated with simple Coulomb glide is unlikely to occur except under very restrictive circumstances. In general axially symmetric motion involves deformation on more than one plane, and will be possible only when two of the principal stresses are equal.⁹ In this paper, attention will be confined to the latter stress state, a more comprehensive discussion being reserved for a forthcoming paper.

Considerable extra freedom of deformation is introduced when two principal stresses are equal. The directions of these two stresses are undefined, and as a consequence glide is possible on all planes tangent to a cone having the third (defined) principal stress direction as axis.

In the case of axial symmetry, it can be shown that a principal strain direction can depart from the defined principal stress direction by an angle $\phi/2$. This result can be demonstrated by computing the strain components in the principal stress directions. Let $3'$, Fig. (2), be the defined principal stress direction. For axial symmetry of stresses, $3'$ will be in the meridional plane unless $\sigma_r = \sigma_z$, a trivial case. Defining $2'$ in the circumferential direction, the principal strain directions 1, 2, 3 will be as shown in Fig. 2 when there is glide on a single plane defined by the angle θ . There will be plane-strain motion in the 1-3 plane, making the angle θ with the $1'3'$ plane, and the direction 3 will deviate $\phi/2$ from $3'$. Let $e_3 = -e = -e_1$. Resolving in the primed directions

$$\begin{aligned}
 e'_{\alpha\beta} &= l_{\alpha i} l_{\beta j} e_{ij} = \sum (l_{\alpha 1} l_{\beta 1} - l_{\alpha 3} l_{\beta 3}) e \\
 &= e \begin{bmatrix} \cos^2\theta \cos\phi & ; & \frac{1}{2} \sin 2\theta \cos\phi & ; & -\cos\theta \sin\phi \\ \frac{1}{2} \sin 2\theta \cos\phi & ; & \sin^2\theta \cos\phi & ; & -\sin\theta \sin\phi \\ -\cos\theta \sin\phi & ; & -\sin\theta \sin\phi & ; & -\cos\phi \end{bmatrix} \quad (6)
 \end{aligned}$$

Now for axially symmetric motion, e'_{22} must be a principal strain, so that $e'_{12} = e'_{23} = 0$; and the various plane motions must combine in such a manner as to meet this condition. The total strain obtained by combining the n strains e_i associated with planes subtending angles θ_i will be

$$e'_{\alpha\beta} = \begin{bmatrix} \cos\phi \sum_1^n e_i \cos^2\theta_i & ; & 0 & ; & -\sin\phi \sum_1^n e_i \cos\theta_i \\ 0 & ; & \cos\phi \sum_1^n e_i \sin^2\theta_i & ; & 0 \\ -\sin\phi \sum_1^n e_i \cos\theta_i & ; & 0 & ; & \cos\phi \sum_1^n e_i \end{bmatrix} \quad (7)$$

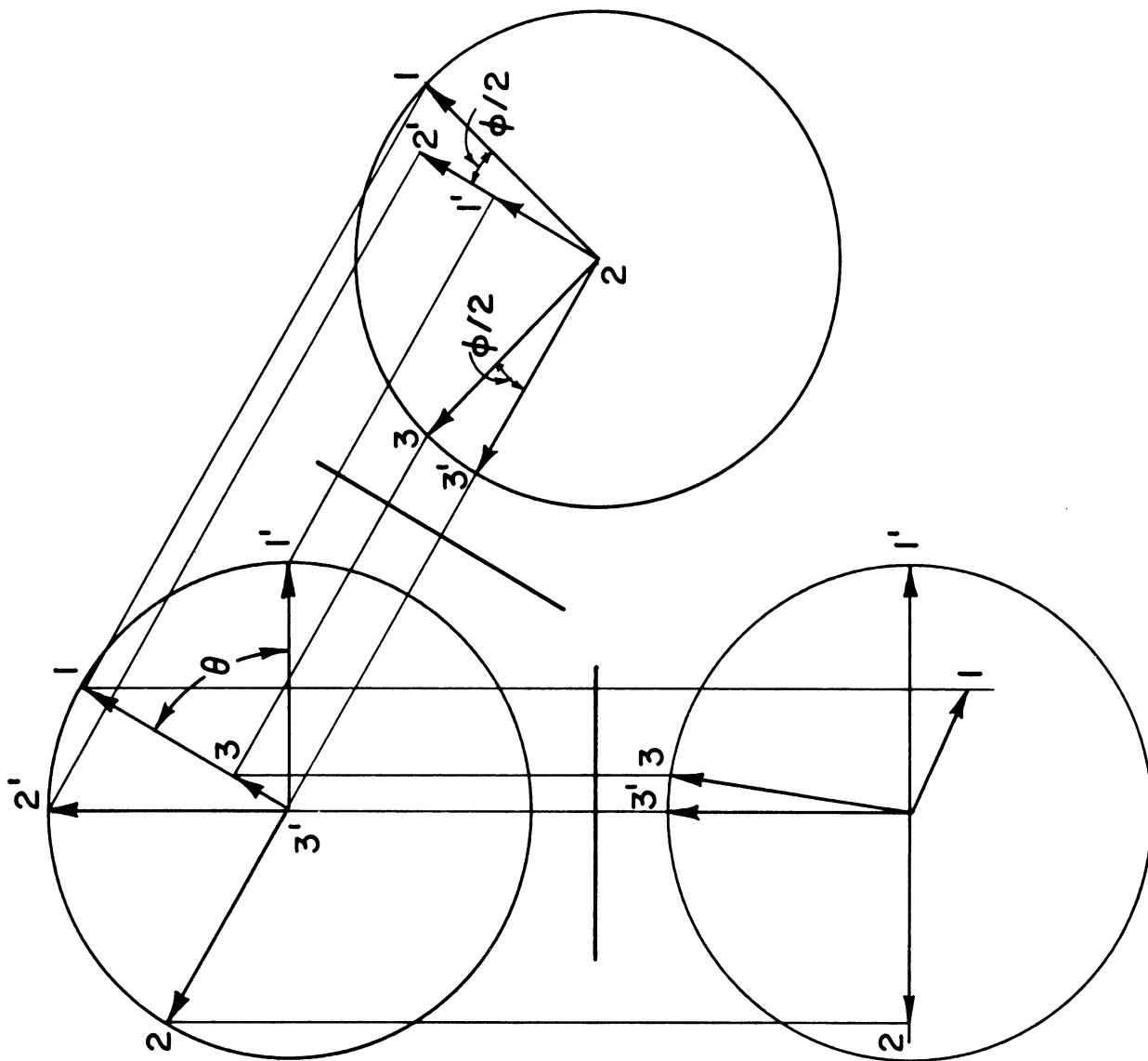


Fig. 2. Unit vectors for two sets of orthogonal axes.

Two principal directions of strain will lie in the meridional plane, one making an angle

$$\frac{1}{2} \tan^{-1} \left(\tan \phi \frac{2 \sum_1^n e_i \cos \theta_i}{\sum_1^n e_i + \sum_1^n e_i \cos^2 \theta_i} \right) \quad (8)$$

with the β' direction. For all θ_i and e_i ,

$$1 \geq \frac{2 \sum_1^n e_i \cos \theta_i}{\sum_1^n e_i + \sum_1^n e_i \cos^2 \theta_i} \geq -1 \quad (9)$$

so that the principal direction of strain does not deviate by more than $\phi/2$ from the principal direction of the stress in the meridional plane. This result will be made use of in an example.

III. THE TRIAXIAL TEST

In the triaxial test, Fig. 3, a cylindrical specimen is compressed between rigid platens while subject to a lateral hydrostatic pressure. The specimen is enclosed in a rubber membrane, so that the intergranular pressure remains atmospheric.

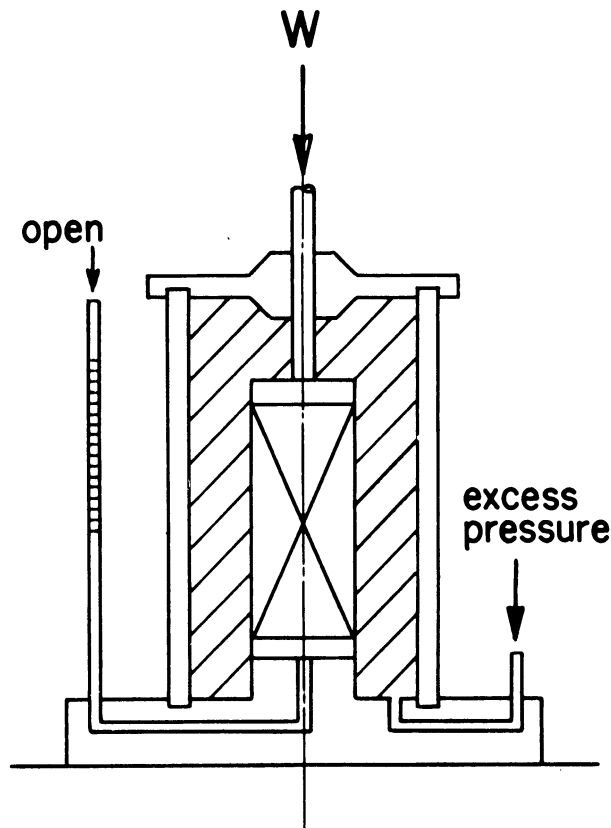


Fig. 3. The triaxial test.

All diametral cross-sections at points remote from the platens may be expected to be stressed in the same manner, at least initially, so that the principal directions of stress will be axial, radial, and circumferential. For radial equilibrium,

$$\frac{d\sigma_r}{dr} + \frac{\sigma_r - \sigma_\theta}{r} = 0 \quad (10)$$

We shall assume tentatively that the circumferential and radial stresses are equal, so that motion will not be restricted to plane strain, and proceed to associate velocity fields with the uniform stress state which results from the substitution $\sigma_r = \sigma_\theta$ in Eq. (10). It should be noted that this procedure, unlike plasticity theory, does not establish uniqueness of the stress state.

A large number of velocity fields can be associated with this stress distribution: two types will be examined for purposes of illustration. Suppose first that a constant angle $\alpha/2$ is maintained between the principal directions of stress and strain rate and where, as established above, the value of α cannot exceed the angle of internal friction ϕ . In the case of axial compression, Fig. 4a, the geometry of the Mohr circle for strain can be defined by the relation

$$\tan\alpha = \frac{\gamma}{e_r - e_z} \quad (11)$$

whereas for axial extension, Fig. 4b,

$$\tan\alpha = \frac{-\gamma}{e_r - e_z} \quad (12)$$

Making use of the definitions

$$-\gamma = \gamma_{rz} = \frac{\partial u}{\partial z} + \frac{\partial w}{\partial r}; \quad e_r = \frac{\partial u}{\partial r}; \quad e_z = \frac{\partial w}{\partial z} \quad (13)$$

the relations between the strain can be written in the form

$$a \frac{\partial u}{\partial r} - \frac{\partial u}{\partial z} - \frac{\partial w}{\partial r} - a \frac{\partial w}{\partial z} = 0 \quad (14)$$

where $a = K \tan\alpha$ and $K = +1$ in the axial compression case and $K = -1$ in the axial extension case. Equation (14) and the zero dilation condition

$$\frac{\partial u}{\partial r} + \frac{u}{r} + \frac{\partial w}{\partial z} = 0 \quad (15)$$

comprise the governing differential equations. In the theory of ideally plastic solids, the corresponding equations are¹⁰:

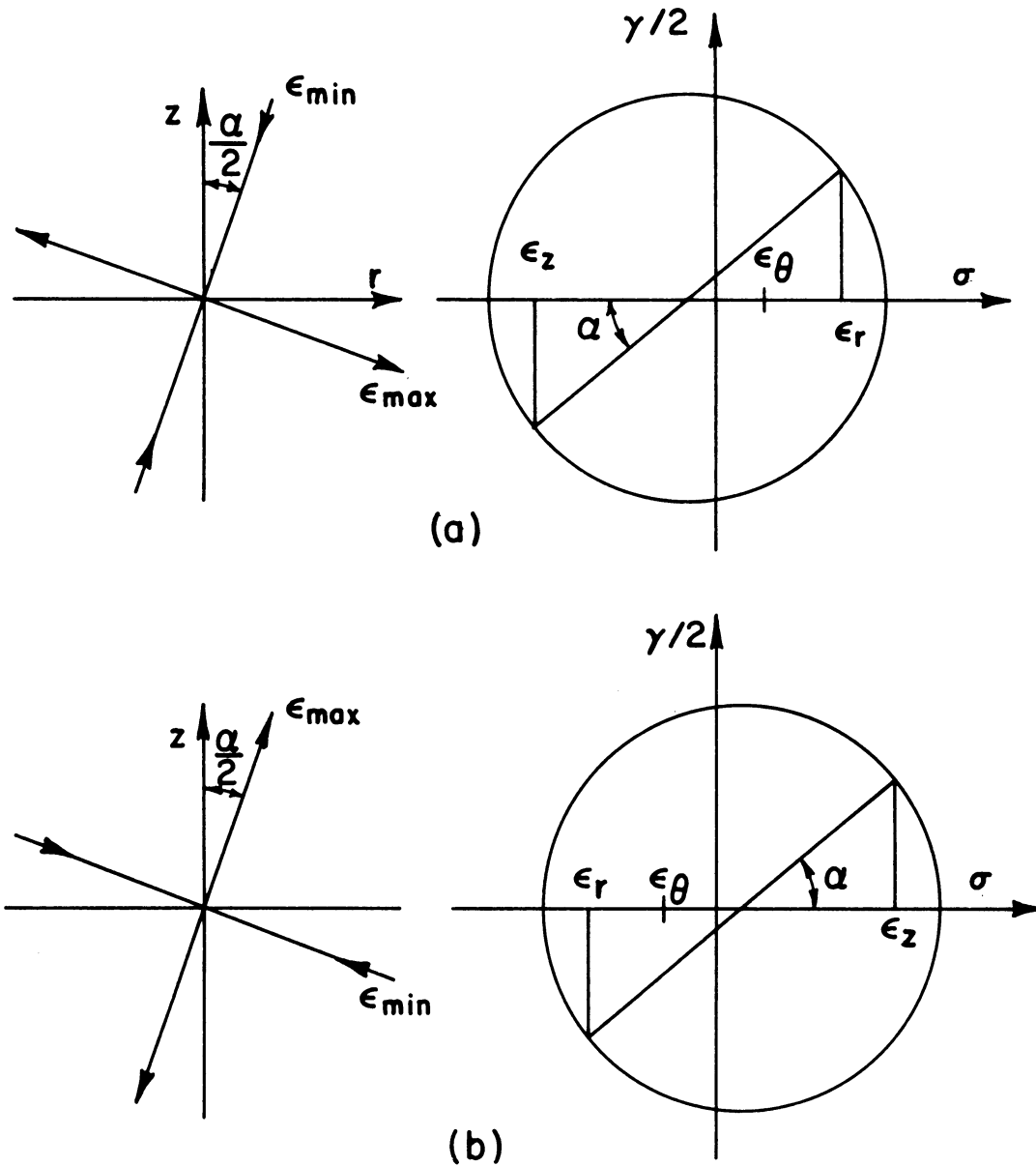


Fig. 4. Strain states for the triaxial test: (a) failure with axial compression; (b) failure with axial extension.

$$\frac{\partial u}{\partial z} + \frac{\partial w}{\partial r} = 0 \quad (16)$$

and

$$\frac{\partial u}{\partial r} + \frac{u}{r} + \frac{\partial w}{\partial z} \tan^2 \left(\frac{\pi}{4} \pm \frac{\phi}{2} \right) = 0 \quad (17)$$

where the positive sign applies for axial compression and the negative for axial extension. Equation (16) is the degenerate form of Eq. (14) on setting $a = 0$, and expresses the fact that, in the plasticity theory, the principal directions of stress and strain rate are assumed to coincide. The analysis makes it clear that Eq. (16) is a necessary condition for isotropy only when the yield criterion of the material is insensitive to the mean stress. Axially symmetric fields satisfying the governing Eqs. (14) and (15) can be found by a technique which parallels closely that used by Shield¹¹ for the compression of ideally plastic metal cylinders. Neither equation involves a fundamental length, so a solution which is independent of length is to be expected, provided suitable velocity-boundary conditions can be found. Writing $\tan \psi = z/r$, Eqs. (14) and (15) reduce to the ordinary differential equations

$$(a \tan \psi + 1) u' - (\tan \psi - a) w' = 0 \quad (18)$$

$$u' \tan \psi - u \sec^2 \psi - w' = 0 \quad (19)$$

where the primes denote differentiation with respect to ψ . Eliminating w' between Eqs. (18) and (19) and employing the substitution $x = \tan \psi$, there results

$$\int \frac{du}{u} = \int \frac{(a - x) dx}{1 + 2ax - x^2} \quad (20)$$

Hence

$$u = C_1 \sqrt{1 + 2ax - x^2} \quad (21)$$

and Eq. (19) can be rewritten

$$\frac{dw}{dx} = \frac{-C_1(ax + 1)}{\sqrt{1 + 2ax - x^2}} \quad (22)$$

For axial compression $a = \tan\alpha$ and

$$u = C_1 \sqrt{(N-x)(1/N+x)} \quad (23)$$

where $N = \tan(\pi/4 + \alpha/2)$. Thus $u = 0$ on the line

$$\psi = \frac{\pi}{4} + \frac{\alpha}{2} \quad (24)$$

which forms a natural boundary to the deforming region. Setting $w = +1$ on $x = 0$ and $w = 0$ on $x = N$, Fig. 5, and integrating Eq. (22), we obtain

$$u = \frac{\cos^2\alpha \sqrt{(N-x)(1/N+x)}}{\frac{\pi}{2} + \alpha - \frac{1}{2} \sin 2\alpha} \quad (25)$$

and

$$w = \frac{\frac{\pi}{2} - \sin^{-1}(x \cos\alpha - \sin\alpha) - \frac{1}{2} \sin 2\alpha \sqrt{(N-x)(1/N+x)}}{\frac{\pi}{2} + \alpha - \frac{1}{2} \sin 2\alpha} \quad (26)$$

For axial extension, $a = -\tan\alpha$ and

$$u = C_1 \sqrt{(N+x)(1/N-x)} \quad (27)$$

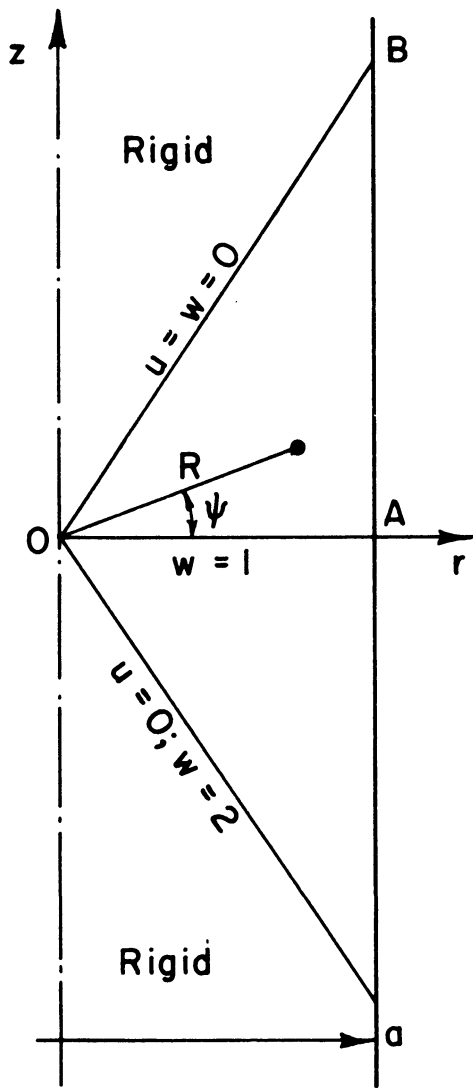
Thus $u = 0$ on the line $\psi = \pi/4 - \alpha/2$, which now forms the natural boundary, Fig. 5b. Setting $w = -1$ on $x = 0$ and $w = 0$ on $x = 1/4$, Fig. 5b, and integrating Eq. (22) we obtain

$$u = \frac{-\sqrt{(N+x)(1/N-x)}}{(1-\tan^2\alpha)(\alpha - \sin^{-1}(1-2\sin\alpha)) + \tan\alpha} \quad (28)$$

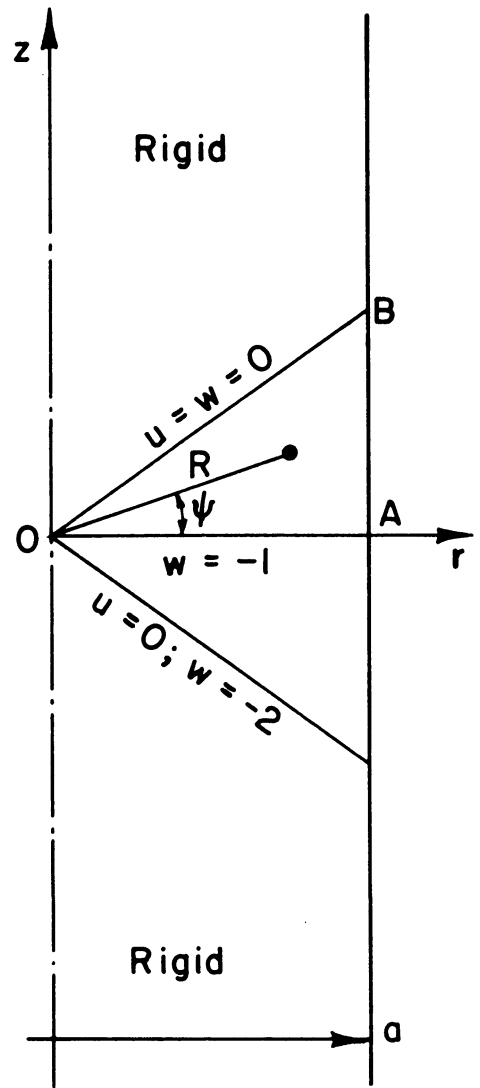
and

$$w = \frac{(1-\tan^2\alpha)(\sin^{-1}(x\cos\alpha - \sin\alpha) - \sin^{-1}(1-2\sin\alpha)) - \tan\alpha \sqrt{(N+x)(1/N-x)}}{(1-\tan^2\alpha)(\alpha - \sin^{-1}(1-2\sin\alpha)) + \tan\alpha} \quad (29)$$

Figure 6a shows the nature of the deformation produced by the velocity field represented by Eqs. (25) and (26) (axial compression) for the case $\phi = 40^\circ$.

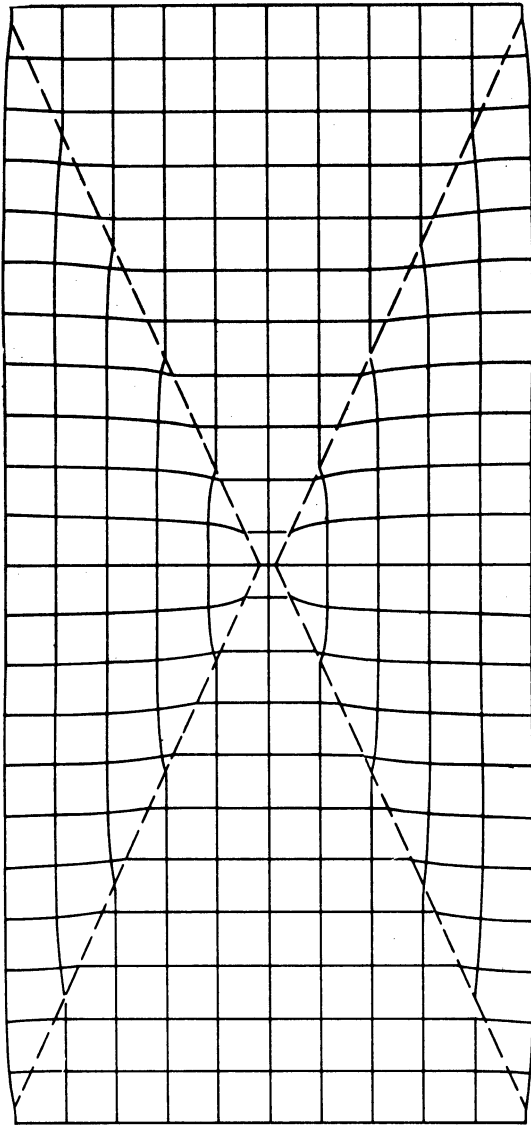


(a)

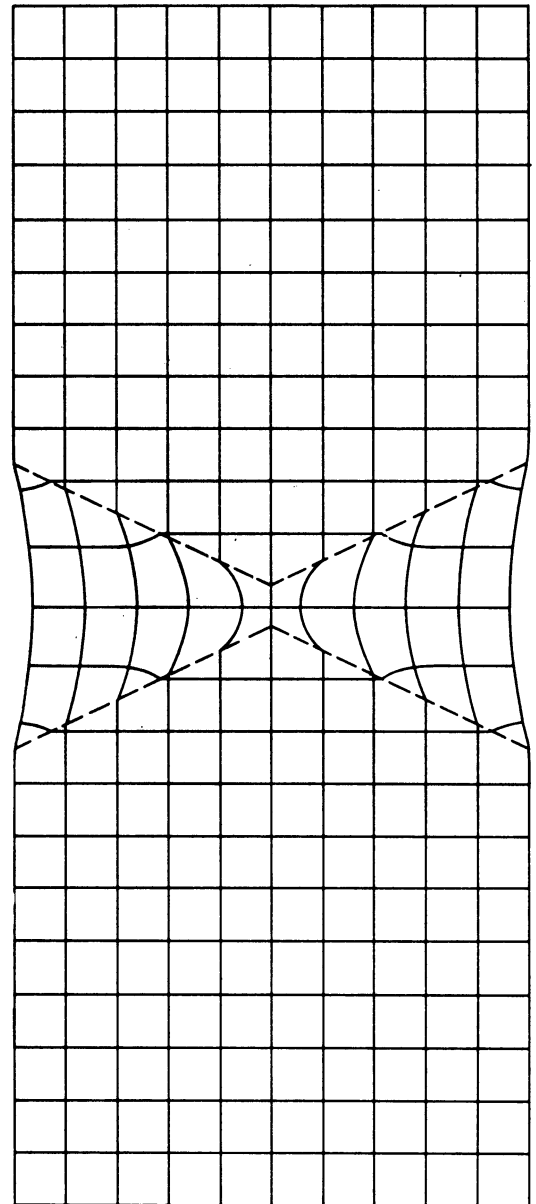


(b)

Fig. 5. Regions of deformation with axial symmetry: (a) failure with axial compression; (b) failure with axial extension.



(a)



(b)

Fig. 6. Distortion of an initially square grid for deformation with axial symmetry; $\alpha = \phi = 40^\circ$: (a) compression failure; (b) extension failure.

Figure 6b shows the deformation for Eqs. (28) and (29) (axial extension).

In the above analysis it was assumed arbitrarily that the angle α was constant throughout the deforming zone. Other solutions for the velocities can be obtained by dropping this assumption. If, for example, all flow in the meridional plane takes place parallel to OB, Fig. 5, then Eq. (14) is replaced by the simple relationship

$$w = Nu \tag{30}$$

The displacement component w can now be eliminated from Eq. (15). Employing the substitution $x = \tan \psi = z/r$ as in the previous case we obtain, after using the boundary condition,

$$w = Nu = 1 - x/N \tag{29}$$

Figure 7 indicates the deformation of an initially square grid in the presence of the velocity field, for the case $\phi = 40^\circ$. The above expressions for displacement all involve the angle α , where $\phi \geq \alpha \geq -\phi$. Evidently the deforming zone can vary between wide limits if there is in fact no further restriction on α , and the actual mode of deformation is likely to be determined by second-order effects, such as the influence of geometry changes on the stress distribution. In the case of axial compression, local deformation will tend to increase the diameter and lower the mean stress so that there will be a tendency, due to this cause above for the strains to extend over the length of the specimen. For axial extension, local strain will reduce the diameter and raise the mean stress, tending to concentrate subsequent deformations in the same zone. Both the above effects are observed; each is consistent with the adoption of $\alpha = \phi$. It is of some interest to speculate that the value $\alpha = \phi$ might always be adopted. New experimental evidence having a bearing on this point is discussed below.

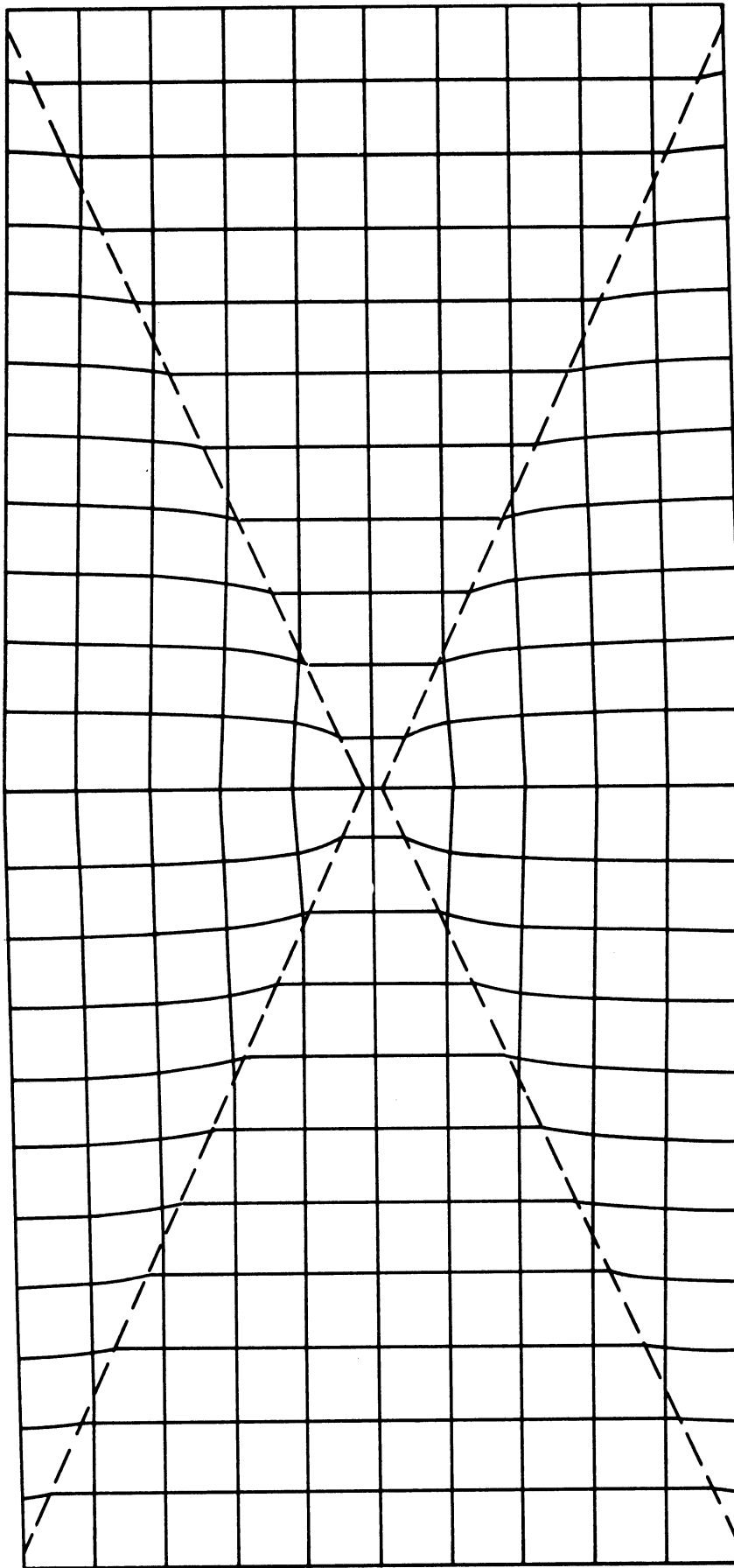


Fig. 7. Distortion of an initially square grid for an alternative velocity field. Compression failure with $\phi = 40^\circ$.

IV. EXPERIMENTAL EVIDENCE

If the Coulomb glide model is accepted without further restrictions, then all the velocity fields developed in the foregoing analysis are possible. Experiment would serve to determine which field is selected in practice, and the process would then be regulated only by second-order effects such as changes in geometry. While such second-order effects undoubtedly develop, and will cause a certain velocity field to be preferred, it is also possible that the Coulomb glide model is not sufficiently restrictive, and that the initial motion is regulated further due to the intrinsic properties of the granular medium. In particular, such a restriction might take the form of limitation to the angle $\alpha/2$ between the principal directions of stress and strain rate. The finding of such a restriction would be most useful in the solution of mixed boundary value problems and it gives a further incentive to the examination of the experimental evidence.

The final shapes of triaxial test specimens are well known, but there seems to be no data available on the incremental behavior during and immediately after the initial deformation. It is quite possible that the final shapes do not reflect the rates of deformation at every stage, and might in fact be misleading. With this point in mind, arrangements were made to take a series of photographs of a triaxial specimen during deformation, so that the rates of deformation of the surface could be estimated.

The test was carried out on a standard triaxial testing machine at Michigan State University. A sample of Ottawa sand 2.8 in. in diameter and 5.2 in. in length was tested in compression under an intergranular vacuum of 11.10 lb/sq in. The use of an intergranular vacuum enabled the enclosing pressure vessel to be dispensed with, which greatly facilitated the photography and eliminated the possibility of optical distortion.

Average rates of radial displacement for two axial displacement increments were found by comparison of photographs under a travelling microscope. The data in Fig. 9a refer to the displacement increment AB, Fig. 8, and that in Fig. 9b to the increment CD, Fig. 8. The average angle of internal friction, computed assuming the internal cohesion to be zero, was 26° ; with $\alpha = \phi$ the deforming zone would then be expected to extend over almost the entire length of the sample, but there is also evidence of a tendency for the deformation to be concentrated towards the bottom of the sample. In Fig. 9b, deformation occurs only at the lower end, over a height very nearly equal to the diameter. The theoretical velocity profile for $\alpha = 0$ (coincidence of the directions of principal stress and strain rate) is indicated by means of the solid lines. The final velocity would appear to conform closely to this theoretical prediction.

The observation that the specimen deformed over almost the entire length

during the early stages cannot be accepted as evidence that the principal directions of stress and strain rate did not coincide, because alternative fields with $\alpha = 0$ exist which are compatible with the data. These have been given by Shield.¹¹ On the other hand, the velocity field in Fig. 9b cannot be reconciled with plasticity theory¹⁰ because it involves too small a depth of the specimen. It has been well known that the dilatation rate predicted by plasticity theory is much too large but until now there has been no example of an inconsistent deformation field available. Now that one has been provided, it lends further weight to the contention that the plasticity theory cannot adequately describe the continuing motion of a granular medium.

One objective of this study was the establishment of some further restriction to the angle α on the basis of experiment. None has emerged; indeed the observations suggest the possibility of wide variations in α during deformation. Thus it appears likely that the actual mode of deformation is determined by factors which have not been considered, such as the influences of soil weight and geometry changes on the stress distribution.

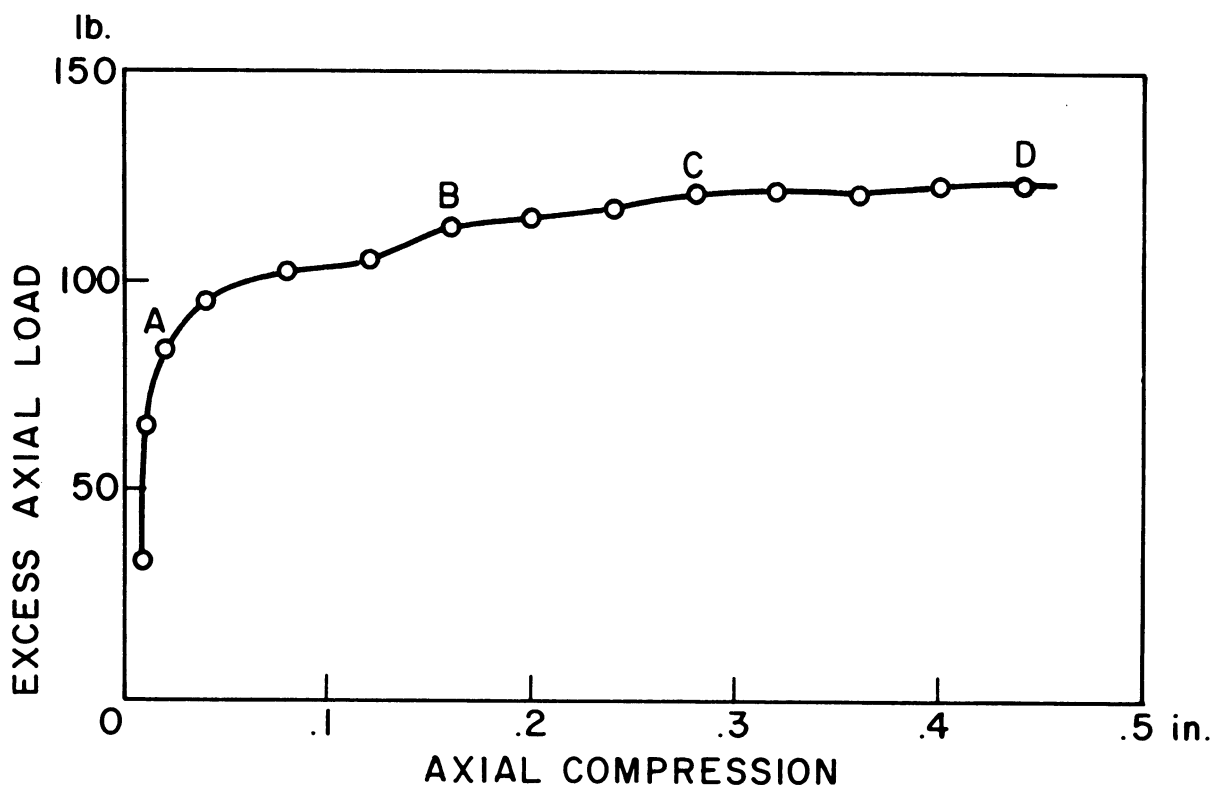
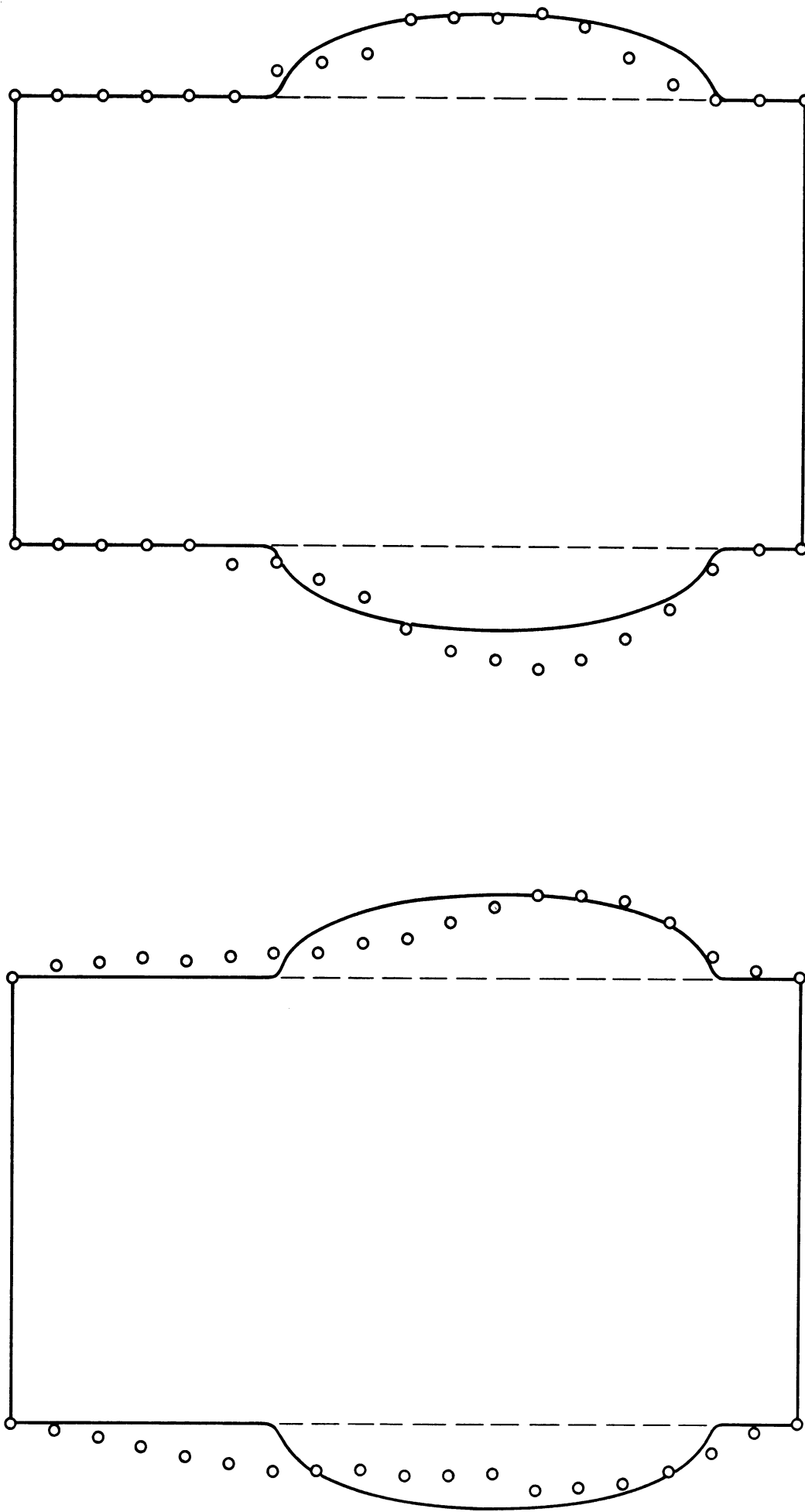


Fig. 8. Load-deflection curve from a triaxial test on Ottawa sand.



(a)

(b)

Fig. 9. Average rates of radial expansion for two increments during the failure of a specimen of Ottawa sand in compression. Circles show experimental points: (a) for the displacement increment AB, Fig. 8, and (b) for the increment CD, Fig. 8. The solid lines show the predicted rates for $\alpha = 0$.

REFERENCES

1. C. A. Coulomb, "Essai sur une Application des Regles des Maximis et Minimis à Quelques Problèmes de Statique, Relatifs à l'Architecture," Mem. Sav. Étr. (Acad. Sci. Paris), Vol. 7, (1773), 343.
2. W. J. M. Rankine, "On the Stability of Loose Earth," Phil. Trans. Roy. Soc. Vol. 147, (1857), pp.9-27.
3. D. C. Drucker and W. Prager, "Soil Mechanics and Plastic Analysis or Limit Design," Quart. Appl. Math., Vol. 10, (1952), pp. 157-165.
4. D. C. Drucker, R. E. Gibson and D. J. Henkel, "Soil Mechanics and Working-Hardening Theories of Plasticity," Trans. Am. Soc. Civil Engrs., Vol. 122, (1957), pp. 338-346.
5. A. W. Jenike and R. T. Shield, "On the Plastic Flow of Coulomb Solids Beyond Original Failure," Trans. Am. Soc. Mech. Engrs., Vol. 26, (1959), Series E (J. Appl. Mech.) pp. 599-602.
6. O. Mohr, "Beiträge zur Theorie des Erddruckes," Z. Arch. u Ing. Ver., Vol. 17, (1871), 344; Vol. 18, (1872), 67, 245.
7. R. M. Haythornthwaite, "Stress and Strain in Soils," pp. 185-192 in Plasticity, ed. E. H. Lee and P. S. Symonds, New York: Pergamon Press Inc., 1960.
8. G. de Josselin de Jong, Statics and Kinematics in the Failable Zone of a Granular Material, Delft: Uitgerij Waltman, 1959.
9. A. Haar and T. v. Kármán, "Zur Theorie der Spannungszustände in plastischen und sandartigen Medien," Nachr Ges. Wiss. Gottingen, Math. Phys. Kl., (1909), pp. 204-218.
10. R. M. Haythornthwaite, "Mechanics of the Triaxial Test for Soils," Proc. Am. Soc. Civil Engrs., Vol. 86, (1960) Series SM, pp. 35-62.
11. R. T. Shield, "On the Plastic Flow of Metals Under Conditions of Axial Symmetry," Proc. Roy. Soc. A., Vol. 233, (1955), pp. 267-286.

<p>AD Accession No. UNCLASSIFIED</p> <p>The University of Michigan, Office of Research Administration, Ann Arbor, Mich. <u>The Kinematics of Soils, by R. M. Haythornthwaite. Report No. 04403-6-T, Aug. 1962, 22 p. incl. illus., Project 04403 (Contract No. DA-20-018-ORD-23276)</u> UNCLASSIFIED</p> <p>A continuum model which provides an adequate representation of the mechanical behavior of a random granular medium such as soil has yet to be discovered. In this paper one candidate—the material which deforms</p> <p style="text-align: right;">(over)</p> <p style="text-align: right;">UNCLASSIFIED</p>	<p>AD Accession No. UNCLASSIFIED</p> <p>The University of Michigan, Office of Research Administration, Ann Arbor, Mich. <u>The Kinematics of Soils, by R. M. Haythornthwaite. Report No. 04403-6-T, Aug. 1962, 22 p. incl. illus., Project 04403 (Contract No. DA-20-018-ORD-23276)</u> UNCLASSIFIED</p> <p>A continuum model which provides an adequate representation of the mechanical behavior of a random granular medium such as soil has yet to be discovered. In this paper one candidate—the material which deforms</p> <p style="text-align: right;">(over)</p> <p style="text-align: right;">UNCLASSIFIED</p>
<p>UNCLASSIFIED</p> <p>by glide on the critical Coulomb friction planes—is used to analyze the kinematics of deformation under conditions of axial symmetry. As in plane strain, the principal directions of stress and strain rate do not necessarily coincide. A detailed analysis is given for the triaxial test and the predicted displacements are compared with some test results for a sand.</p> <p style="text-align: right;">UNCLASSIFIED</p>	<p>UNCLASSIFIED</p> <p>by glide on the critical Coulomb friction planes—is used to analyze the kinematics of deformation under conditions of axial symmetry. As in plane strain, the principal directions of stress and strain rate do not necessarily coincide. A detailed analysis is given for the triaxial test and the predicted displacements are compared with some test results for a sand.</p> <p style="text-align: right;">UNCLASSIFIED</p>

<p>AD Accession No. UNCLASSIFIED</p> <p>The University of Michigan, Office of Research Administration, Ann Arbor, Mich. <u>The Kinematics of Soils, by R. M. Haythornthwaite. Report No. 04403-6-T, Aug. 1962, 22 p. incl. illus., Project 04403 (Contract No. DA-20-018-ORD-23276)</u> UNCLASSIFIED</p> <p>A continuum model which provides an adequate representation of the mechanical behavior of a random granular medium such as soil has yet to be discovered. In this paper one candidate—the material which deforms (over)</p> <p style="text-align: right;">UNCLASSIFIED</p>	<p>AD Accession No. UNCLASSIFIED</p> <p>The University of Michigan, Office of Research Administration, Ann Arbor, Mich. <u>The Kinematics of Soils, by R. M. Haythornthwaite. Report No. 04403-6-T, Aug. 1962, 22 p. incl. illus., Project 04403 (Contract No. DA-20-018-ORD-23276)</u> UNCLASSIFIED</p> <p>A continuum model which provides an adequate representation of the mechanical behavior of a random granular medium such as soil has yet to be discovered. In this paper one candidate—the material which deforms (over)</p> <p style="text-align: right;">UNCLASSIFIED</p>
<p>UNCLASSIFIED</p> <p>AD Accession No. UNCLASSIFIED</p> <p>The University of Michigan, Office of Research Administration, Ann Arbor, Mich. <u>The Kinematics of Soils, by R. M. Haythornthwaite. Report No. 04403-6-T, Aug. 1962, 22 p. incl. illus., Project 04403 (Contract No. DA-20-018-ORD-23276)</u> UNCLASSIFIED</p> <p>A continuum model which provides an adequate representation of the mechanical behavior of a random granular medium such as soil has yet to be discovered. In this paper one candidate—the material which deforms (over)</p> <p style="text-align: right;">UNCLASSIFIED</p>	<p>UNCLASSIFIED</p> <p>by glide on the critical Coulomb friction planes—is used to analyze the kinematics of deformation under conditions of axial symmetry. As in plane strain, the principal directions of stress and strain rate do not necessarily coincide. A detailed analysis is given for the triaxial test and the predicted displacements are compared with some test results for a sand.</p> <p style="text-align: right;">UNCLASSIFIED</p>

